Journal of Clinical Monitoring and Computing (2010) 24:413–419
DOI: 10.1007/s10877-010-9263-z

HOW DO CHANGES IN EXHALED CO_2 MEASURE CHANGES IN CARDIAC OUTPUT? A NUMERICAL ANALYSIS MODEL

Peter H. Breen, MD, FRCPC

Breen PH. How do changes in exhaled CO_2 measure changes in cardiac output? A numerical analysis model.
J Clin Monit Comput 2010; 24:413–419

ABSTRACT. Objective. In a previous study in anesthetized animals, the slope of percent decreases in exhaled CO_2 versus percent decreases in cardiac output ($\dot{Q}_T$, inflation of vena cava balloons) was 0.73. To examine the mechanisms underlying this exhaled CO_2-$\dot{Q}_T$ relationship, an iterative numerical analysis computer model of non-steady state CO_2 kinetics was developed. **Methods.** The model consisted of a large peripheral tissue compartment connected by venous return and $\dot{Q}_T$ to a small central pulmonary compartment. Equations were developed to describe the movement of CO_2 in this system. Decreases in $\dot{Q}_T$ were accompanied by experimentally measured increases in alveolar dead space fraction ($V_{D_{alv}}/V_{T_{alv}}$), generated by decreased pulmonary vascular pressure during the $\dot{Q}_T$ decrease. **Results.** When the model was perturbed by a 40% decrease in $\dot{Q}_T$ and an increase in $V_{D_{alv}}/V_{T_{alv}}$ from 5 to 20.6%, average alveolar expired P_{CO_2} ($P\overline{AE}_{CO_2}$) decreased from 37.5 to 29.4 mm Hg, similar to the animal experiments. Due to the high peripheral tissue compliance for CO_2, the computer model demonstrated that, after a decrease in $\dot{Q}_T$, at least 1 h was required for compartment CO_2 stores to approach a new equilibrium state. **Conclusions.** The numerical analysis computer model helps to delineate the mechanisms underlying how decreased $\dot{Q}_T$ resulted in decreased exhaled CO_2. The model permitted deconvolution of the effects of simultaneous variables and the interrogation of parameters that would be difficult to measure in actual experiments.

KEY WORDS. non-steady state, carbon dioxide, numerical analysis, computer modeling, alveolar dead space, blood transport of CO_2, cardiac output.

INTRODUCTION

In the classical, steady state alveolar gas equation, $F_{A_{CO_2}} = \dot{V}_{CO_2,ti}/\dot{V}_A$, where $F_{A_{CO_2}}$ is the alveolar fraction of CO_2, $\dot{V}_{CO_2,ti}$ is the tissue production of CO_2, and $\dot{V}_A$ is alveolar ventilation. Cardiac output ($\dot{Q}_T$) does not appear in the equation, although it transports CO_2 from the tissues to the lung [1]. During steady state, blood CO_2 transport equals $\dot{V}_{CO_2,ti}$. In recent years, there has been increased understanding of the clinical relationships between $\dot{Q}_T$ and exhaled CO_2 during non-steady state [1]. Disastrous cardiovascular events during anesthesia (e.g. severe hypovolemia) result in the exponential decrease of end-tidal P_{CO_2} ($P_{ET_{CO_2}}$) within about ten breaths [2]. Reports during cardiopulmonary resuscitation [3, 4] demonstrate that changes in $P_{ET_{CO_2}}$ can reflect changes in $\dot{Q}_T$. Indeed, the best signal of the return of spontaneous circulation (with marked increase in $\dot{Q}_T$ and venous

From the Department of Anesthesiology and Perioperative Care, University of California-Irvine, UCI Medical Center, Building 53, Room 227, Orange, CA 92868, USA.

Received 31 December 2008. Accepted for publication 12 October 2010.

Address correspondence to P. H. Breen, Department of Anesthesiology and Perioperative Care, University of California-Irvine, UCI Medical Center, Building 53, Room 227, Orange, CA 92868, USA.
E-mail: pbreen@uci.edu

return) during cardiopulmonary resuscitation may be the significant increase in $P_{ET_{CO_2}}$ [5].

In a previous study of anesthetized dogs [6], $\dot{Q}_T$ was decreased by variable inflation of superior and inferior vena cava balloons. Over a range of acute decreases in $\dot{Q}_T$, the plot of percent decrease in PET_{CO2} versus percent decrease in $\dot{Q}_T$ yielded a slope of 0.73. Two mechanisms were proposed to explain how an abrupt decrease in $\dot{Q}_T$ decreases PET_{CO_2}. First, the reduction in venous return decreases the transport of CO_2 from tissues to lung. In the face of constant minute ventilation ($\dot{V}_E$), alveolar P_{CO_2} (PA_{CO_2}) will decrease. Second, the alveolar dead space fraction of alveolar tidal volume (VD_{alv}/VT_{alv}) will increase due to the reduced pulmonary vascular pressure that occurs during a decrease in $\dot{Q}_T$ [7, 8]. This increase in VD_{alv} will dilute and decrease PET_{CO_2} below PA_{CO_2} [9]. During a sustained reduction in $\dot{Q}_T$, recovery of exhaled CO_2 will result from the accumulation of CO_2 in the peripheral tissue compartment and resultant increase in mixed venous P_{CO_2} ($P\bar{v}_{CO_2}$). The increase in $P\bar{v}_{CO_2}$ restores CO_2 transport to the lung, increases PA_{CO2}, and, hence, pulmonary CO_2 elimination. In fact, PA_{CO2} must rise above the baseline value to restore pulmonary CO_2 elimination ($\dot{V}_{CO_2}$) to equal the tissue $\dot{V}_{CO_2}$ because $\dot{V}_A$ was decreased by the increase in VD_{alv}/VT_{alv}.

To help examine and validate these hypotheses, I have developed a numerical analysis model of non-steady state CO_2 kinetics. I perturb this computer model with an abrupt decrease in $\dot{Q}_T$, examine the resultant time course and changes in CO_2 kinetics variables, and compare the model predictions with the experimentally measured changes.

METHODS AND MATERIALS

Overview of the numerical analysis model of non-steady state CO_2 kinetics

The computer model consists of a large peripheral tissue compartment of CO_2 stores and a small central pulmonary compartment of CO_2 stores [10, 11] (Figure 1). The peripheral tissue compartment is connected by venous return and $\dot{Q}_T$ to the central pulmonary compartment. CO_2 is transported in arterial and venous blood, as governed by its solubility relationships (see below). $\dot{V}_{CO_2,ti}$ adds to the peripheral CO_2 compartment. $\dot{V}_A$, which equals $\dot{V}_E$ minus the effects of anatomical dead space (VD_{ana}) and VD_{alv}, eliminates CO_2 from the central pulmonary compartment. The alveolar-capillary membrane, across which gas exchange occurs, is depicted by the dotted line. VD_{alv}, which does not participate in gas exchange, is separated from pulmonary capillary blood by the solid line. The numerical algorithms assume that the addition of high ventilation-to-alveolar perfusion ($\dot{V}_A/\dot{Q}$) regions, where alveolar corner vessels may remain open [12], are represented by alveolar dead space (VD_{alv}) ($\dot{V}_A/\dot{Q}$ equal to infinity) for modeling convenience.

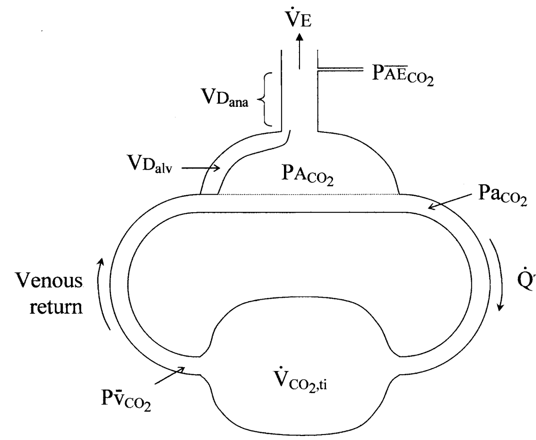

Fig. 1. Scheme of CO_2 kinetics. The large, peripheral tissue compartment of CO_2 stores is connected by venous return and cardiac output ($\dot{Q}_T$) to the small, central pulmonary compartment of CO_2 stores. Tissue CO_2 production ($\dot{V}_{CO_2,ti}$) adds to the peripheral CO_2 compartment. Alveolar ventilation ($\dot{V}_A$), which equals minute ventilation ($\dot{V}_E$) minus the effects of anatomical dead space (VD_{ana}) and alveolar dead space (VD_{alv}), eliminates CO_2 from the central pulmonary compartment. The alveolar-capillary membrane, across which gas exchange occurs, is depicted by the dotted line. VD_{alv}, which does not participate in gas exchange, is separated from pulmonary capillary blood by the solid line. Average alveolar expired P_{CO_2}($P\overline{AE}_{CO_2}$) is measured at the airway opening. (During clinical anesthesia, the less accurate end-tidal P_{CO_2} (PET_{CO_2}) is usually measured instead of $P\overline{AE}_{CO_2}$). PA_{CO_2}, alveolar P_{CO_2}; Pa_{CO_2}, arterial blood P_{CO_2}; $P\bar{v}_{CO_2}$, mixed venous blood P_{CO_2}.

Tidal P_{CO_2} is measured at the airway opening and $P\overline{AE}_{CO_2}$ is determined. $P\overline{AE}_{CO_2}$ is the average alveolar P_{CO_2} normalized for exhaled volume [13]. In other words, $P\overline{AE}_{CO_2}$ is the mean P_{CO_2} value of the alveolar plateau of the CO_2 expirogram (plot of exhaled P_{CO_2} versus exhaled volume). During clinical anesthesia, the less accurate PET_{CO_2} is usually measured instead of $P\overline{AE}_{CO_2}$. PET_{CO_2} is the P_{CO_2} of the last exhaled alveolar gas sampled at the airway opening. In other words, PET_{CO_2} is the final P_{CO_2} value of the alveolar plateau of the capnogram (plot of exhaled P_{CO_2} versus time).

Iterative computer model

The numerical analysis is an iterative process in which the following consecutive events are evaluated during each iterative period (usually 1 s):

1. *Change in CO_2 volume of the central pulmonary compartment* equals *CO_2 transport in blood* minus *CO_2 elimination from lung*.
2. *Change in $P_{A_{CO_2}}$* equals *Change in CO_2 volume of the central pulmonary compartment* divided by *pulmonary CO_2 compliance*.
3. $P\overline{AE}_{CO_2}$ equals $P_{A_{CO_2}} \cdot (1 - V_{D_{alv}}/V_{T_{alv}})$ [6, 13] (re-arrangement of the equation for alveolar dead space fraction).
4. *Change in CO_2 volume of the peripheral tissue compartment* equals $\dot{V}_{CO_2,ti}$ minus *CO_2 transport in blood*.
5. *Change in $P\bar{v}_{CO_2}$* equals *Change in CO_2 volume of the peripheral tissue compartment* divided by *tissue CO_2 compliance*.

Specific parameters of the CO_2 kinetics model

Table 1 displays the independent and dependent variables of the CO_2 kinetics model, scaled for the body weight of the dog. Blood CO_2 content (C_{CO_2}) is calculated from P_{CO_2} assuming a linear CO_2 blood solubility relationship (ml $CO_2 \cdot 100$ ml blood$^{-1} \cdot$ mm Hg $P_{CO_2}^{-1}$) [14–16] and the Haldane effect [17–19]. The Haldane effect, which describes the increase in CO_2 blood content when hemoglobin desaturates, accounts for 46% of total CO_2 transfer. The CO_2 compliance of the peripheral tissues (ml CO_2/mm Hg P_{CO_2}) was determined from tissue weight [20] and the slope of the tissue dissociation curve for CO_2 [10, 15]. The CO_2 compliance of the venous blood compartment was determined from the volume of venous blood [20] and the CO_2 blood solubility. The CO_2 compliance of the pulmonary gas compartment depends on the functional residual capacity (FRC). The CO_2 compliance of the lung tissue [14] accounts for storage of CO_2 in actual lung parenchyma. The CO_2 compliance of the arterial blood compartment was determined from the volume of arterial blood [20] and the CO_2 blood solubility. Other canine baseline variables were taken from measurements in our laboratory [7, 21].

Table 1. Initial independent and dependent variables in the CO_2 kinetics mathematical model in the dog (baseline data for Fig. 3)

Independent variables	
$\dot{Q}_T$ (l/min)	2.5
$\dot{V}_E$ (l/min)	3.2
$F_{I_{CO_2}}$	0.0
$V_{D_{ana}}/V_T$ (%)	30
$V_{D_{alv}}/V_{T_{alv}}$ (%)	5
$\dot{V}_{CO_2,ti}$ (ml/min)	120
P_B (mm Hg)	747
P_{H_2O} (mm Hg)	47
CO_2 blood solubility (ml %/mm Hg P_{CO_2})	0.45
Haldane effect (ml %)	2.21
CO_2 Compliance$_{\text{Peripheral Tissue}}$ (ml CO_2/mm Hg P_{CO_2})	53.0
CO_2 Compliance$_{\text{Venous Blood}}$ (ml CO_2/mm Hg P_{CO_2})	4.50
CO_2 Compliance$_{\text{FRC}}$ (ml CO_2/mm Hg P_{CO_2})	1.43
CO_2 Compliance$_{\text{Arterial Blood}}$ (ml CO_2/mm Hg P_{CO_2})	2.10
CO_2 Compliance$_{\text{Lung Tissue}}$ (ml CO_2/mm Hg P_{CO_2})	0.55
Dependent variables	
Total V_D/V_T (%)	33.5
$\dot{V}_A$ (l/min)	2.13
$P_{A_{CO_2}}$ (mm Hg)	39.5
$P\overline{AE}_{CO_2}$ (mm Hg)	37.5
Pa_{CO_2} (mm Hg)	39.5
$P\bar{v}_{CO_2}$ (mm Hg)	45.2

$\dot{Q}_T$, cardiac output (equal to venous return); $\dot{V}_E$, minute ventilation; $F_{I_{CO_2}}$, fraction of inspired CO_2; $V_{D_{ana}}/V_T$, anatomical dead space fraction of total tidal volume; $V_{D_{alv}}/V_{T_{alv}}$, alveolar dead space fraction of total alveolar volume; $\dot{V}_{CO_2,ti}$, tissue CO_2 production; P_B, barometric pressure; P_{H_2O}, water vapor partial pressure in alveolar gas; FRC, functional residual capacity; $\dot{V}_A$, alveolar ventilation; $P_{A_{CO_2}}$, alveolar P_{CO_2}; $P\overline{AE}_{CO_2}$, average alveolar expired P_{CO_2}; Pa_{CO_2}, arterial blood P_{CO_2}; $P\bar{v}_{CO_2}$, mixed venous blood P_{CO_2}; "ml %" is ml CO_2 per 100 ml blood.For explanations and formulas, see the text section, *Specific Parameters of the CO_2 Kinetics Model,* in the *Methods and Materials*.

Experimental perturbations of the CO_2 kinetics mathematical model

Figure 2 displays the *Data|BreakPoints* page of the computer model. From the baseline model data displayed in Table 1, $\dot{Q}_T$ is decreased by 1 l/min (40% decrease) over 5 s beginning at 10 s of the 130 s model simulation run (Figure 3). The simultaneous increase in $V_{D_{alv}}/V_{T_{alv}}$ of 15.6% (=40% $\cdot$ 0.39) is calculated from the slope of the change in $V_{D_{alv}}/V_{T_{alv}}$ versus percent decrease in $\dot{Q}_T$ (0.39), measured in the canine study [6]. The maximum acute changes in variables were measured in the model at 65 s, to correspond with the temporal measurement sequence conducted in the canine study. This sequence was repeated over a range of percent decreases in $\dot{Q}_T$ from 10 to 80% to generate Figure 4. Finally, the simulation run depicted in Figures 2 and 3 was extended to 3,615 s to seek the time required to restore equilibrium to the CO_2 kinetics system (Figure 5).

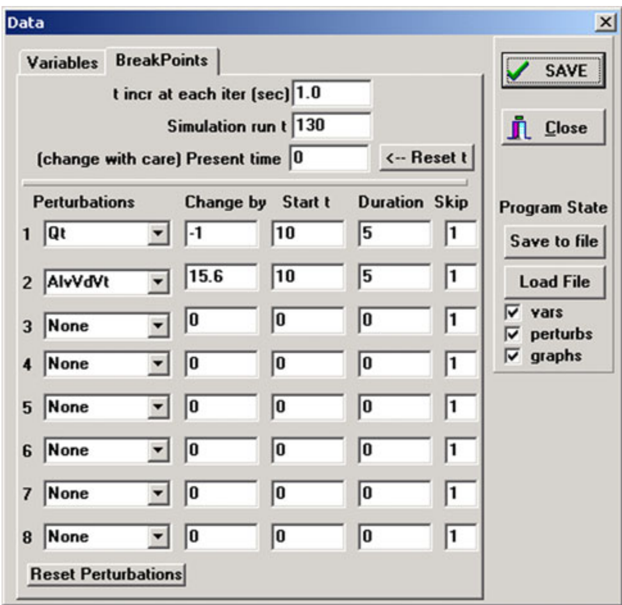

Fig. 2. Data input screen of the CO_2 kinetics computer model. The BreakPoints page allows up to 8 independent perturbations of model variables. The displayed perturbations of cardiac output (Qt, l/min) and alveolar dead space-to-tidal volume ratio (AlvVdVt, %) generate the data shown in Figure 3. For example, at 10 s of the model run, Qt will decrease by 1 l/min over 5 s. The Skip parameter of 1 indicates that the change in Qt will be applied to consecutive time increments. t incr at each iter is the time increment during each iteration of the model. The Variables page (not shown) provides user inspection and access to all of the variables shown in Table 1 (baseline data for Figure 3). Program State save feature allows the complete disk file storage of the state of the program, including model variables, perturbations, and graph settings.

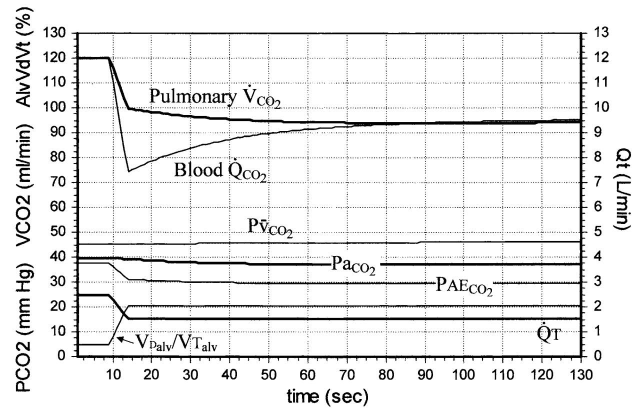

Fig. 3. CO_2 kinetics model: acute decrease in cardiac output. From the baseline condition displayed in Table 1, at 10 s, cardiac output ($\dot{Q}_T$) decreased from 2.5 to 1.5 l/min and the alveolar dead space fraction (V_{Dalv}/V_{Talv}) increased from 5 to 20.6%. The numerical analysis calculated the displayed variables every sec up to a total simulation time of 130 s. $P\overline{AE}_{CO_2}$ average alveolar expired P_{CO_2}; Pa_{CO_2}, arterial blood P_{CO_2}; $P\bar{v}_{CO_2}$, mixed venous blood P_{CO_2}; pulmonary $\dot{V}_{CO_2}$, CO_2 elimination from the lung by alveolar ventilation (ml/min); blood $\dot{Q}_{CO_2}$, CO_2 transport in blood from the peripheral tissue compartment to lung.

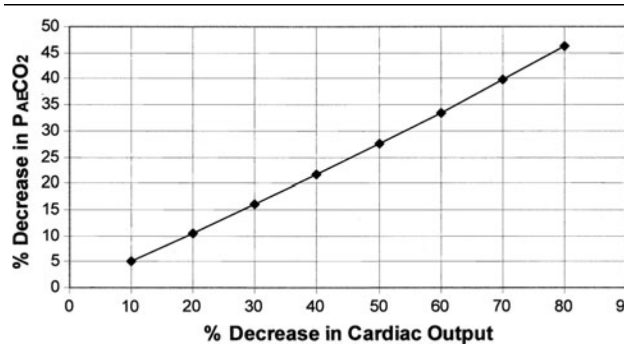

Fig. 4. CO_2 kinetics model predictions of percent decreases in average alveolar expired P_{CO_2} ($P\overline{AE}_{CO_2}$) versus percent decreases in cardiac output ($\dot{Q}_T$). For each simulation run, the baseline condition variables values are displayed in Table 1 and V_{Dalv}/V_{Talv} was increased according to (% decrease in $\dot{Q}_T$) · 0.39 (see Figure 2 and text for details). Analysis by linear regression yielded a slope of 0.59, y-intercept of −1.4, and R^2 of 0.998.

RESULTS

The computer model simulation run in Figure 3 began from the baseline condition displayed in Table 1. The perturbation began at 10 s, consisting of a 40% decrease in $\dot{Q}_T$ from 2.5 to 1.5 l/min and an increase in V_{Dalv}/V_{Talv} from 5 to 20.6% over 5 s. During the 5 s perturbation, $P\overline{AE}_{CO_2}$ decreased abruptly from 37.5 to 31.1 mm Hg and pulmonary $\dot{V}_{CO_2}$ decreased from 120.0 to 103.9 ml/min; at 65 s of simulation time, $P\overline{AE}_{CO_2}$ and pulmonary $\dot{V}_{CO_2}$ had decreased to 29.4 mm Hg and 94.2 ml/min, respectively. The perturbation resulted in a steady decrease in arterial blood P_{CO_2} (Pa_{CO_2}) from 39.5 mm Hg at baseline to 37.0 mm Hg at 65 s of simulation time. During the same period, $P\bar{v}_{CO_2}$ (tissue P_{CO_2}) steadily increased from 45.2 to 45.8 mm Hg.

For eight simulation runs (as depicted in Figure 3) over a range of decreases in $\dot{Q}_T$, Figure 4 plots the percent decreases in $P\overline{AE}_{CO_2}$ versus the percent decreases in $\dot{Q}_T$. The points lie almost on a straight line, with only slight upward convexity. Linear regression yields a slope of 0.59, y-intercept of −1.4, and coefficient of determination (R^2) of 0.998.

Figure 5 extends Figure 3 (40% decrease in $\dot{Q}_T$ from 2.5 to 1.5 l/min and increase in V_{Dalv}/V_{Talv} from 5 to 20.6%) to a simulation time of 3,615 s. By 1 h (3,600 s), pulmonary $\dot{V}_{CO_2}$ had increased back to 115.7 ml/min, compared with the baseline value of 120.0 ml/min. In an analogous fashion, $P\overline{AE}_{CO_2}$ and Pa_{CO_2} had increased back to 36.2 and 45.5 mm Hg, respectively, compared with the baseline values of 37.5 and 39.5 mm Hg, respectively.

By 1 h, $P\bar{v}_{CO_2}$ had increased to 57.8 mm Hg, compared with the baseline value of 45.2 mm Hg.

DISCUSSION

Acute decrease in cardiac output: effects on CO_2 kinetics

During a 40% decrease in $\dot{Q}_T$ from 2.5 to 1.5 l/min (with concurrent increase in $V_{D_{alv}}/V_{T_{alv}}$ from 5 to 20.6%), the numerical analysis of CO_2 kinetics predicted a 21.6% decrease in $P\overline{AE}_{CO_2}$ from 37.5 to 29.4 mm Hg and a 21.5% decrease in pulmonary $\dot{V}_{CO_2}$ from 120 to 94.2 ml/min (Figure 3). These results were similar to the representative animal sequence presented in the canine study of non-steady state decreases in $\dot{Q}_T$ [6], where $P_{ET_{CO_2}}$ decreased from 38 to 28 mm Hg and pulmonary $\dot{V}_{CO_2}$ decreased from 155 to 108 ml/min, when $\dot{Q}_T$ was decreased from 2.8 to 1.5 l/min. When 32 sequences of decreased $\dot{Q}_T$ were analyzed in the canine study, the slope of percent decreases in $P_{ET_{CO2}}$ (or percent decreases in pulmonary $\dot{V}_{CO_2}$) versus percent decreases in $\dot{Q}_T$ was near 0.74. The computer model predicted a slope of 0.59 (Figure 4).

Why did the computer model of CO_2 kinetics predict a lower slope for the plot of percent decreases in exhaled CO_2 versus percent decreases in $\dot{Q}_T$? I propose that the experimental determination of $V_{D_{alv}}/V_{T_{alv}}$ was falsely low during a decrease in $\dot{Q}_T$ [6]. The experimental study used $P_{ET_{CO2}}$ (from the capnogram) and not $P\overline{AE}_{CO_2}$ (from the CO_2 expirogram) as the estimate of $P_{A_{CO2}}$. Because of the normal positive slope of the alveolar plateau, $P_{ET_{CO2}}$ will be higher than $P\overline{AE}_{CO_2}$ [11, 13]. Furthermore, during the decrease in $\dot{Q}_T$, an increase in $\dot{V}_A/\dot{Q}$ heterogeneity may have occurred and further increased the slope of the alveolar plateau [22]. Thus, the over-estimation of Pa_{CO_2} by $P_{ET_{CO_2}}$ would have under-estimated the determination of $V_{D_{alv}}/V_{T_{alv}}$, given by $\left(Pa_{CO_2} - P_{A_{CO_2}}\right)/P_{A_{CO_2}}$. Then, these experimentally determined falsely low values of $V_{D_{alv}}/V_{T_{alv}}$ were used to perturb the computer model and resulted in smaller predicted decreases in exhaled CO_2 during a given decrease in $\dot{Q}_T$.

In the canine study of decreased $\dot{Q}_T$ [6], data was presented as percent changes in exhaled CO_2 versus percent changes in $\dot{Q}_T$, rather than comparing arithmetic changes in these variables. The rationale for this data analysis approach stated that, at a lower starting $\dot{Q}_T$, a given $\dot{Q}_T$ decrease should cause a larger decrease in exhaled CO_2 because a larger fractional reduction in CO_2 delivery would occur. The numerical analysis of CO_2 kinetics supports this contention. In the computer model, baseline $\dot{Q}_T$ was changed from 2.5 to 2.0 l/min and the system was iterated to a new equilibrium. After perturbing this baseline state with the same range of percent decreases in $\dot{Q}_T$ (and associated changes in $V_{D_{alv}}/V_{T_{alv}}$), the slope of the plot of percent changes in exhaled CO_2 versus percent decreases in $\dot{Q}_T$ (Figure 4) was still 0.59.

The numerical analysis approach allows the examination of parameters and physiology that would be difficult to measure experimentally. In Figure 3, when the perturbation decreased $\dot{Q}_T$ and increased $V_{D_{alv}}/V_{T_{alv}}$, note that blood CO_2 transport $\left(\dot{Q}_{CO_2}\right)$ from tissues to lung decreased much more than the decrease in pulmonary $\dot{V}_{CO_2}$. The decrease in blood $\dot{Q}_{CO_2}$ was caused almost entirely by the decrease in $\dot{Q}_T$. However, the effect of the $\dot{Q}_T$ decrease to decrease pulmonary $\dot{V}_{CO_2}$ was initially buffered by the "release" of CO_2 from the central pulmonary compartment CO_2 stores [6, 10, 15].

The numerical analysis approach can help deconvolute the effects of simultaneous changes in variables. For example, removing the increase in $V_{D_{alv}}/V_{T_{alv}}$ from the perturbation in Figure 3 (i.e. perturbation only decreases $\dot{Q}_T$) eliminates the abrupt decreases in $P\overline{AE}_{CO_2}$ and pulmonary $\dot{V}_{CO_2}$. These indices of exhaled CO_2 depend on $\dot{V}_A$, which is immediately decreased by the increase in $V_{D_{alv}}$. In contrast, the absence of the increase in $V_{D_{alv}}$ does not change the character of the steady decrease in Pa_{CO_2}. Interestingly, at 65 s of the simulation run, Pa_{CO_2} was 1.7 mm Hg *lower* because $\dot{V}_A$ is higher, compared to the simulation condition which includes the increase in $V_{D_{alv}}$.

Sustained decrease in cardiac output: effects on CO_2 kinetics

Figure 5 continues the simulation from Figure 3 ($\dot{Q}_T$ decrease from 2.5 to 1.5 l/min and $V_{D_{alv}}/V_{T_{alv}}$ increase from 5 to 20.6%) to 1 h. By 1 h after the perturbation, CO_2 kinetics variables had significantly recovered towards a new equilibrium. Pulmonary $\dot{V}_{CO_2}$ was 115.7 ml/min (baseline value was 120 ml/min). The decrease in $\dot{V}_A$ (due to increased $V_{D_{alv}}$) caused a general increase in CO_2 body stores [6, 10]. However, the decrease in $\dot{Q}_T$ resulted in a redistribution of CO_2 stores towards the peripheral tissue compartment—note that $P\bar{v}_{CO_2}$ (tissue P_{CO_2}) increased more than Pa_{CO_2}.

This numerical analysis prediction of the time course of CO_2 kinetics after a sustained decrease in $\dot{Q}_T$ is similar to experimentally measured data in animals. In the canine study of decreased $\dot{Q}_T$ [6], in three dogs the pulmonary $\dot{V}_{CO_2}$ had recovered to 81% of the baseline value by 25 min of sustained inflation of the vena cava balloons, compared to the computer model prediction of 90% recovery (Figure 5). Similarly, in another animal study, 11 cm H_2O positive end-expiratory pressure (PEEP)

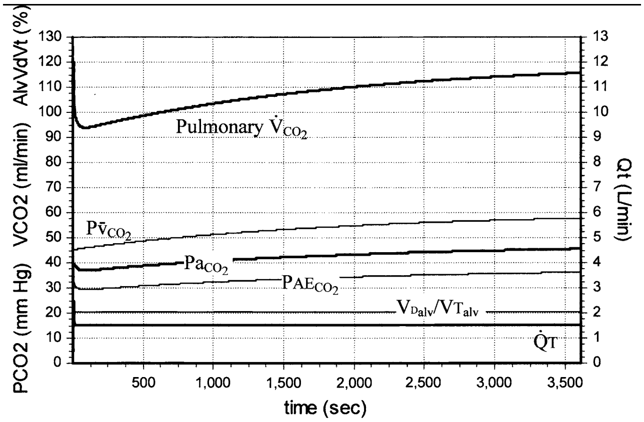

Fig. 5. CO_2 kinetics model: sustained decrease in cardiac output (extension of the simulation run of Figure 3 from 130 to 3,615 s). From the baseline condition displayed in Table 1, at 10 s, cardiac output ($\dot{Q}T$) decreased from 2.5 to 1.5 l/min and the alveolar dead space fraction (V_{Dalv}/V_{Talv}) increased from 5 to 20.6%. $P\overline{AE}_{CO_2}$, average alveolar expired P_{CO_2}; Pa_{CO_2}, arterial blood P_{CO_2}; $P\bar{v}_{CO_2}$, mixed venous blood P_{CO_2}; pulmonary $\dot{V}_{CO_2}$, CO_2 elimination from the lung by alveolar ventilation (ml/min).

resulted in decreased $\dot{Q}T$ and increased physiological dead space [11]. After 25 min of PEEP, pulmonary $\dot{V}_{CO_2}$ had recovered to 82% of the baseline (pre-PEEP) value. In contrast, in a study of anesthetized patients where application of 10 cm H_2O PEEP caused an acute reduction in $\dot{Q}T$ [23], by 20 min of PEEP, pulmonary $\dot{V}_{CO_2}$ had recovered to 95% of the baseline value because $\dot{Q}T$ also recovered to its baseline value.

These changes in CO_2 kinetics variables after the perturbation highlight the large peripheral tissue stores of CO_2 [10, 15, 20]. Although bone is by far the largest CO_2 store in the body [10], it is excluded from the analysis because it equilibrates slowly and should not affect experiments whose duration is only an hour or so [15]. These modeling considerations assume constant tissue $\dot{V}_{CO_2}$ and $\dot{V}E$ [6].

Innovations of the numerical analysis computer model of CO_2 kinetics

Traditional mathematical models of CO_2 kinetics invoke the simultaneous solution of differential equations [10] or the use of electrical analogues [15, 20]. In contrast, the numerical analysis model described in this paper incorporates an iterative approach, where objects (composed of variables and equations) in the program define the different elements in the system of CO_2 kinetics. Then, at each iterative interval, these objects interact with each other and change their values accordingly, just like the body. A perturbation to the system is applied over a set duration (Figure 2), because an instantaneous change in a variable could upset the system, as well as being non-physiologic.

The advantages of an iterative mathematical model include the following: (1) The difficult and tedious task of solving simultaneous differential equations is avoided. Numerous, independent, and asynchronous perturbations of different variables can be applied to the iterative computer model (Figure 2), resulting in complex changes to the CO_2 kinetics system, which essentially precludes the approach of solution of differential equations. (2) The numerical analysis model allows the interrogation of variables that are difficult or impossible to measure (e.g. blood $\dot{Q}_{CO_2}$ from tissues to lung). (3) The computer model allows the deconvolution of the effects of simultaneous changes in variables (e.g. separating the effects of $\dot{Q}T$ decrease and VD_{alv} increase in Figure 3). (4) The computer model can generate simulation experiments to test hypotheses that are too difficult to control in an animal model and that are not appropriate for a patient study.

The program was written in Delphi Pascal (version 5.0, Inprise Corporation). Full use was made of object-oriented programming techniques (encapsulation, inheritance, and polymorphism). The rich array of Delphi input and output services facilitate a robust user interface that maximizes the utility of the model. For example, the user can click on graph plots to interrogate y-values and time-values. Graphs can be exported to enhanced metafiles (*.wmf files, Windows operating system, Microsoft, Redmond, Washington) for presentation or manuscript preparation.

Limitations of the numerical analysis computer model of CO_2 kinetics

The computer model incorporates a number of physiological simplifications. A linear CO_2 dissociation relationship in blood is assumed. Interactions of O_2 are limited to a simple Haldane effect, which increases CO_2 content in deoxygenated blood. The range of $\dot{V}A/\dot{Q}$ relationships in the lung is reduced to a simple two-compartment model (normal alveolar compartment and VD_{alv}), where the numerical algorithms assume that the addition of high ventilation-to-alveolar perfusion ($\dot{V}A/\dot{Q}$) regions, where alveolar corner vessels may remain open [12], are represented by alveolar dead space (V_{Dalv}) ($\dot{V}A/\dot{Q}$ equal to infinity). The peripheral tissues are considered to be one homogenous compartment.

Yet, even with these constraints, the above description and use of the numerical analysis of CO_2 kinetics establishes its ability to test hypotheses, discern underlying mechanisms, and predict data to formulate new hypotheses. In fact, the simple model, as long as it can adequately simulate the physiologic system, is more elegant and inter-relationships of variables are easier to understand. In addition, a simple model executes quickly and has the ability to be programmed into a hand-held calculator or into a spreadsheet program.

Finally, any constraint conferred by the above limitations is simply an invitation to extend the numerical analysis model. The Pascal structured, object-oriented programming approach lends itself to extensibility of the numerical analysis model.

This work was supported by NIH Grant HL-42637 from the National Heart, Lung, and Blood Institute.

REFERENCES

1. Breen PH. Carbon dioxide kinetics during anesthesia: pathophysiology and monitoring. In: Breen PH, editor. Respiration in anesthesia: pathophysiology and clinical update. Philadelphia: WB Saunders, Anesthesiology Clinics North America 1998; 16: 259–93.
2. Swedlow DB. Capnometry and capnography: the anesthesia disaster early warning system. Seminars Anesth 1986; 5: 194–205.
3. Falk JL, Rackow EC, Weil MH. End-tidal carbon dioxide concentration during cardiopulmonary resuscitation. N Eng J Med 1988; 318: 607–611.
4. Garnett A, Ornato JP, Gonzalez ER, Johnson B. End-tidal carbon dioxide monitoring during cardiopulmonary resuscitation. JAMA 1987; 257: 512–515.
5. Trevino RP, Bisera J, Weil MH, Rackow EC, Grundler WG. End-tidal CO_2 as a guide to successful cardiopulmonary resuscitation: a preliminary report. Crit Care Med 1985; 13: 910–911.
6. Isserles SA, Breen PH. Can changes in end-tidal P_{CO2} measure changes in cardiac output?. Anesth Analg 1991; 73: 808–814.
7. Breen PH, Schumacker PT, Hedenstierna G, Ali J, Wagner PD, Wood LDH. How does increased cardiac output increase shunt in pulmonary edema?. J Appl Physiol 1982; 53: 1273–1280.
8. West JB, Dollery DT, Naimark A. Distribution of blood flow in isolated lung; relation to vascular and alveolar pressures. J Appl Physiol 1964; 19: 713–724.
9. Nunn JF, Hill DW. Respiratory dead space and arterial to end-tidal CO_2 tension difference in anesthetized man. J Appl Physiol 1960; 15: 383–389.
10. Cherniack NS, Longobardo GS. Oxygen and carbon dioxide gas stores of the body. Physiol Rev 1970; 50: 196–243.
11. Breen PH, Mazumdar B. How does positive end-expiratory pressure decrease CO_2 elimination from the lung?. Respir Physiol 1996; 103: 233–242.
12. Hedenstierna G, White FC, Mazzone R, Wagner PD. Redistribution of pulmonary blood flow in the dog with PEEP ventilation. J Appl Physiol 1979; 46: 278–287.
13. Breen PH, Mazumdar B, Skinner SC. Comparison of end-tidal P_{CO_2} and average alveolar expired P_{CO_2} during positive end-expiratory pressure. Anesth Analgesia 1996; 82: 368–373.
14. Sackner MA, Feisal KA, DuBois AB. Determination of tissue volume and carbon dioxide dissociation slope of the lungs in man. J Appl Physiol 1964; 19: 374–380.
15. Farhi LE, Rahn H. Dynamics of changes in carbon dioxide stores. Anesthesiology 1960; 21: 604–614.
16. Farhi LE. Gas stores of the body. In: Fenn WO, Rahn H, eds, Handbook of physiology: Respiration (Section 3, Volume 1, Chapter 34). American Physiology Society, Washington, DC, 1964: 873–885.
17. Hill EP, Power GG, Longo LD. Kinetics of O_2 and CO_2 exchange. In: West JB, editor. Bioengineering aspects of the lung. Lung biology in health and disease, Vol 3. New York: Dekker; 1977; 459–514.
18. Klocke RA. Carbon dioxide transport. In: Farhi, LE, Tenney, SM, eds, Handbook of physiology, The Respiratory System (Vol 4: Gas Exchange). American Physiology Society, Bethesda, 1987: 173–197.
19. Christiansen J, Douglas CC, Haldane JS. The absorption and dissociation of carbon dioxide by the human blood. J Physiol (London) 1914; 48: 244–271.
20. Whelpton D. Models of carbon dioxide stores in man. In: Thornton JA, editor. The use of computers for anesthesia teaching, Boston: Little, Brown, & Co, Intl Anesthesiol Clinics; 1971; 9: 109–123.
21. Breen PH, Becker L, Ruygrok P, Mayers I, Long GR, Leff A, Wood LDH. Canine bronchoconstriction, gas trapping, and hypoxia with methacholine. J Appl Physiol 1987; 63: 262–269.
22. West JB, Fowler KT, Hugh-Jones P, O'Donnell TV. The measurement of the inequality of ventilation and of perfusion in the lung by the analysis of single expirates. Clin Sci 1957; 16: 549–565.
23. Johnson JL, Breen PH. How does positive end-expiratory pressure decrease pulmonary CO_2 elimination in anesthetized patients? Respir Physiol 1999; 118: 227–236.